Different contribution of conserved amino acids to the global properties of Triosephosphate isomerases

ARTICLE *in* PROTEINS STRUCTURE FUNCTION AND BIOINFORMATICS · FEBRUARY 2014

Impact Factor: 2.63 · DOI: 10.1002/prot.24398 · Source: PubMed

11 AUTHORS, INCLUDING:

Yolanda Aguirre
Universidad Nacional Autónoma de México
1 PUBLICATION **3** CITATIONS
SEE PROFILE

Alejandra Hernandez-Santoyo
Universidad Nacional Autónoma de México
28 PUBLICATIONS **305** CITATIONS
SEE PROFILE

Reyes Vivas
Instituto Nacional de Pediatría
43 PUBLICATIONS **417** CITATIONS
SEE PROFILE

Miguel Costas
Universidad Nacional Autónoma de México
104 PUBLICATIONS **2,049** CITATIONS
SEE PROFILE

PROTEINS
STRUCTURE ■ FUNCTION ■ BIOINFORMATICS

Different contribution of conserved amino acids to the global properties of triosephosphate isomerases

Yolanda Aguirre,[1] Nallely Cabrera,[1] Beatriz Aguirre,[1] Ruy Pérez-Montfort,[1] Alejandra Hernandez-Santoyo,[2] Horacio Reyes-Vivas,[3] Sergio Enríquez-Flores,[3] Marietta Tuena de Gómez-Puyou,[1] Armando Gómez-Puyou,[1]* Jose M. Sanchez-Ruiz,[4]* and Miguel Costas[5]*

[1] Departamento de Bioquímica y Biología Estructural, Instituto de Fisiología Celular, Universidad Nacional Autónoma de México, México D.F, México

[2] Instituto de Química, Universidad Nacional Autónoma de México, México D.F, México

[3] Laboratorio de Bioquímica-Genética, Torre de Investigación, Instituto Nacional de Pediatría, Secretaría de Salud, 04530, México, D.F, México

[4] Departamento de Química Física, Facultad de Ciencias, Universidad de Granada, Granada, Spain

[5] Laboratorio de Biofisicoquímica, Departamento de Fisicoquímica, Facultad de Química, Universidad Nacional Autónoma de México, México D.F, México

ABSTRACT

It is generally assumed that the amino acids that exist in all homologous enzymes correspond to residues that participate in catalysis, or that are essential for folding and stability. Although this holds for catalytic residues, the function of conserved noncatalytic residues is not clear. It is not known if such residues are of equal importance and have the same role in different homologous enzymes. In humans, the E104D mutation in triosephosphate isomerase (TIM) is the most frequent mutation in the autosomal diseases named "TPI deficiencies." We explored if the E104D mutation has the same impact in TIMs from four different organisms (*Homo sapiens, Giardia lamblia, Trypanosoma cruzi*, and *T. brucei*). The catalytic properties were not significantly affected by the mutation, but it affected the rate and extent of formation of active dimers from unfolded monomers differently. Scanning calorimetry experiments indicated that the mutation was in all cases destabilizing, but the mutation effect on rates of irreversible denaturation and transition-state energetics were drastically dependent on the TIM background. For instance, the E104D mutation produce changes in activation energy ranging from 430 kJ mol^{-1} in HsTIM to −78 kJ mol^{-1} in TcTIM. Thus, in TIM the role of a conserved noncatalytic residue is drastically dependent on its molecular background. Accordingly, it would seem that because each protein has a particular sequence, and a distinctive set of amino acid interactions, it should be regarded as a unique entity that has evolved for function and stability in the organisms to which it belongs.

Proteins 2014; 82:323–335.

Key words: kinetic stability; transition-state plasticity; protein denaturation; free-energy barriers; homologous enzymes.

INTRODUCTION

One of the concepts that have derived from the analysis of amino acid sequence of numerous proteins is that the conservation of an amino acid or an amino acid sequence in homologous proteins is related to its functional importance. According to this view, it is expected that a mutation of a conserved residue would yield an enzyme with impaired catalytic activity or low stability. Although modifications of catalytic residues indeed affect enzyme catalysis, the function and contribution of other residues that are conserved throughout the biological scale to the global properties of proteins are not entirely

Additional Supporting Information may be found in the online version of this article.

Grant sponsor: Consejo Nacional de Ciencia y Tecnologia de Mexico (CONACyT); grant numbers: 99844-Q (to M.C.); 167823 (to R.P.M.); Grant sponsor: Dirección General de Asuntos del Personal Académico (PAPIIT-UNAM); grant numbers: IN221812 (to R.P.M.); IN112813 (to M.C.); Grant sponsor: Spanish Ministry of Science and Innovation; grant numbers: BIO2012–34937; CSD2009-00088; Grant sponsor: FEDER Funds (to J.M.S.-R.).

*Correspondence to: Armando Gómez-Puyou, Departamento de Bioquímica y Biología Estructural, Instituto de Fisiología Celular, Universidad Nacional Autónoma de México, México D.F., México. E-mail: apuyou@ifc.unam.mx (or) Jose M. Sanchez-Ruiz, Departamento de Química Física, Facultad de Ciencias, Universidad de Granada, Granada, Spain. E-mail: sanchezr@ugr.es (or) Miguel Costas, Laboratorio de Biofisicoquímica, Departamento de Fisicoquímica, Facultad de Química, Universidad Nacional Autónoma de México, México D.F., México. E-mail: costasmi@unam.mx

Received 11 March 2013; Revised 30 July 2013; Accepted 14 August 2013
Published online 22 August 2013 in Wiley Online Library (wileyonlinelibrary.com).
DOI: 10.1002/prot.24398

clear. This is because the folding, function, and structure of proteins are determined by a network of interactions of each amino acid with neighboring and distant residues,[1–6] indicating that even in proteins with a high level of identity and similarity, the direct contacts and long-range interactions that a conserved amino acid establishes may not be the same in distinct homologous enzymes. Hence, a conserved residue may contribute differently to the overall properties of different homologous enzyme.

To gain insight into this issue, we have studied the E104D mutation in triosephosphate isomerase (TIM), a ubiquitous enzyme that catalyzes the interconversion between glyceraldehyde-3-phosphate and dihydroxyacetone phosphate.[7,8] The enzyme is a homodimer that is catalytically active only in its dimeric form.[9,10] Although seemingly innocuous, the E104D mutation is the most frequent mutation responsible for human TIM deficiency, a rare autosomal disease that leads to premature death in homozygotes.[11–13] In this respect, it has been reported that affected individuals display reduced levels of TIM activity, most likely caused by the strongly decreased stability of the E104D mutant.[14] However, it is not at all clear how a mutation involving two very similar amino acids can have such a dramatic effect on TIM stability. In fact, it could be that the strong effect of the mutation in human TIM (HsTIM) is linked to the particular molecular structure of the human TIM. To examine this possibility, we compared the effect of E104D mutation on the characteristics of TIMs of four organisms that are either close or far in the evolutionary scale: *Trypanosoma cruzi*, *Trypanosoma brucei*, *Giardia lamblia* (TcTIM, TbTIM, and GlTIM, respectively), and HsTIM. The wild types of the four enzymes have comparable catalytic properties, share the classical $(\alpha/\beta)_8$ barrel structure, and the RMS between their crystal structures is around 0.9 Å.[14–17] However, the four enzymes differ in the number of amino acids in their respective monomers: HsTIM and TbTIM have 250 residues, TcTIM has 251 (the extra residue being at the beginning of the sequence), and GlTIM has 256 residues (relative to HsTIM, it has two extra residues at positions 155 and 156, and four additional amino acids in its C-terminal region). For simplicity, in this work all mutants are referred to as E104D. In addition, it is noted that the amino acid identity between TcTIM and TbTIM is 73%, whereas those of TcTIM and TbTIM with HsTIM are 49 and 52%, respectively. GlTIM is 45% identical with HsTIM, and 47% and 45% with TcTIM and TbTIM, respectively. Thus, the four enzymes provide a good model to ascertain the effect of the E104D mutation on distinct molecular contexts.

The catalytic properties of the E104D mutants were similar to those of the respective wild type. However, in the four enzymes the mutation affected dimer formation from unfolded monomers, albeit to different extents. The thermal stabilities of the enzymes and mutants were examined by differential scanning calorimetry (DSC). In all cases, the mutation caused destabilization, but it was also found that the mutation affected the kinetic stability of the four enzymes. It is relevant, however, that the effect of the mutation was drastically different in each of the four enzymes. The overall data thus show that the impact of the E104D mutation depends on the particular molecular settings that arose in the course of evolution of the $(\alpha/\beta)_8$ barrel structure.

MATERIALS AND METHODS

Site-directed mutagenesis, protein expression, and purification

The mutants E104DTbTIM and E105DTcTIM were constructed from the wild-type plasmids containing TbTIM and TcTIM, respectively.[18,19] Codons GAG and GAA coding for a Glu residue in positions 104 of TbTIM and 105 of TcTIM, respectively, were changed to the GAT triplet, coding for Asp, by means of the QuikChange protocol (Stratagene) using Vent DNA polymerase (New England Biolabs) and the sequences: forward: 5′-CGCGCATACTATGGT*GAT*ACAAACGAGATTGTTGCG-3′ and reverse: 5′-CGCAACAATCTCGTTTGT*ATC*ACCATAGTATGCGCG-3′ for E104DTbTIM and forward: 5′-GTTTGTACTACGGC*GAT*ACGAACGAAATCGTTGC-3′ and reverse: 5′-GCAACGATTTCGTTCGT*ATC*GCCGTAGTACAAAC-3′ for E105DTcTIM.

The plasmids were transformed into *Escherichia coli* strain BL21(DE3) pLys (Novagen). The plasmid with HsTIM was transformed into BL21-CodonPlus (-DE3) RIL (Stratagene). Cells were grown at 37°C in LB medium containing ampicillin until reaching an $A_{600\ nm}$ of 0.8–1.2. At that time, they were induced overnight with 0.4 m*M* isopropyl β-D−1-thiogalactopyranoside. The recombinant wild-type and mutant proteins were purified according to Garcia-Torres *et al.*[3]

The recombinant mutant enzyme E104DHsTIM, and HsTIM were produced and purified as described in Rodríguez-Almazán *et al.*[14] The enzyme C202AGlTIM (referred in this article as GlTIM) was prepared as described by Enriquez-Flores *et al.*[20] The GlTIM experiments were conducted with the C202A mutant that forms stable dimers. The C202A mutation does not have appreciable effects on the catalytic properties,[17] and is located on the surface of enzyme and at 27.6 Å of the E104 residue (distance between C_α). Therefore, no appreciable contacts between these two residues were observed.[17] E105DC202AGlTIM (referred in this article as E104DGlTIM) was constructed by site directed PCR mutagenesis using as template mutant C202AGlTIM. The mutagenic oligonucleotides were forward: 5′-AAGACG CAGAATCATGGGG*GAT*ACCGACGAGCAAAGCGCC-3′

and reverse: 5′-GGCGCTTTGCTCGTCGGT*ATC*CCC-CATGATTCTGCGTCTT-3′. The external oligonucleotides were T7 promoter and T7 terminator (Novagen). The mutation was introduced using the following PCR protocol: 94°C for 4 min, 25 cycles for 1 min at 94°C, 1 min at 57°C, 1 min at 72°C, and 10 min at 72°C. Automated DNA sequencing of the complete genes confirmed successful mutagenesis. The PCR products were cloned into the pET-HisTEVP plasmid after digestion with *Nde*I and *Bam*HI, which introduces a $(His)_6$-tag and a tobacco etch virus protease (TEVP) recognition sequence at the amino-terminal portion of the protein.

Protein expression and purification were performed as described previously,[14,18–20] with some modifications. Briefly, BL21(DE3)-pLysS cells with the corresponding pET-HisTEVP-TIM plasmid were grown at 37°C in LB medium plus 100 mg/L ampicillin until an $OD_{600\ nm}$ of 0.6 was reached. Expression was induced overnight with 0.4 m*M* isopropyl β-D-galactopyranoside at 30°C. Cells were harvested by centrifugation and resuspended in lysis buffer containing 50 m*M* NaH_2PO_4, 300 m*M* NaCl, and 10 m*M* imidazole, pH 8.0. Cells were maintained at 4°C, disrupted by sonication and centrifuged at 45,000 RPM for 1 h. The supernatant was added to a 5 × 5 mL His Trap HP column (GE Healthcare) and eluted with an imidazole gradient (0–500 m*M*). The eluted protein was added to a Hi Prep 26/10 Desalting column (GE Healthcare) in 50 m*M* Tris HCl, 0.5 m*M* ethylenediaminetetraacetic acid (EDTA), 1 m*M* dithiothreitol (DTT), pH 8, which is the appropriate buffer for the TEPV enterokinase activity. The eluted enzyme was incubated overnight at 30°C with TEVP at a ratio of 20 GlTIM/1 TEVP (w/w). The digested proteins were then added to a Hi Prep 26/10 Desalting column (GE Healthcare) in a buffer containing 50 m*M* NaH_2PO_4, 300 m*M* NaCl, and 10 m*M* imidazole, pH 8.0 and the eluted sample separated in the His Trap HP column (GE Healthcare). This last step removes the $(His)_6$-tag from the GlTIMs (wild type or mutant), as well as the $(His)_6$-TEPV. The wild type and the mutants were concentrated to 8 mg/mL with Amicon Ultra filters 30,000 MWCO (Millipore) and dialyzed overnight in 100 m*M* triethanolamine (TEA), 1 m*M* EDTA, and 1 m*M* DTT. The yield for the various enzymes ranged from 20 to 35 mg/L.

Enzyme activity

Enzyme activity was measured in the direction of glyceraldehyde-3-phosphate to dihydroxyacetone phosphate, at 25°C. The reaction mixture had 100 m*M* TEA, 10 m*M* EDTA, pH 7.4, 1 m*M* glyceraldehyde-3-phosphate, 0.2 m*M* NADH, and 0.9 units of α-glycerophosphate dehydrogenase. The reaction was initiated by addition of 5 ng/mL of protein. NADH oxidation was monitored at 340 nm in a Hewlett-Packard spectrophotometer. To calculate the kinetic parameters, glyceraldehyde-3-phosphate concentration was varied between 0.06 and 2 m*M*.

Reactivation of the enzymes

The enzymes were denatured by incubation with 6*M* guanidinium hydrochloride (GdnHCl) for 1 h at 25°C at a concentration of 500 μg/mL in a buffer containing 100 m*M* TEA and 10 m*M* EDTA (pH 7.4). For reactivation of the enzymes, aliquots of the latter mixture were diluted 100-fold into media that contained 100 m*M* TEA, 10 m*M* EDTA, and 1 m*M* DTT, pH 7.4. After dilution, aliquots were withdrawn at different times and added to the reaction mixture for activity measurements.

Crystallization conditions

Drops were mixed in a 1:1 volume ratio (v/v) of the recombinant enzyme (3.5 mg/mL in a buffer solution containing 20 m*M* TEA, 10 m*M* EDTA, pH 7.4) and the precipitant solutions (0.01*M* nickel (II) chloride hexahydrate, 0.1*M* Tris pH 8.6, 25% w/v PEG monomethyl ether 2000) from condition H9 of Crystal screen I (Hampton Research™). The crystals were obtained in drops incubated for 2 weeks. Data were collected at the Southeast Regional Collaborative Access Team (SER-CAT) 22-ID beamline at the Advanced Photon Source (Argonne National Laboratory), using a MarMosaic MX-300 detector. The dataset were indexed and integrated with XDS[21] and scaled with SCALA.[22,23]

Structure determination and refinement

Initial phases for the TcTIM E104D and TbTIM E104D structures were determined by the molecular replacement method with the program Phaser v.2.1,[24] using the atomic coordinates of the native TcTIM (PDB code: 1TCD) and TbTIM (PDB code: 2J27) as search models. All the refinement steps were performed using PHENIX.[25] The initial molecular replacement solutions were refined using rigid-body refinement and then non-crystallographic symmetry (NCS) restraints were applied. The resulting models underwent iterative cycles of refinement and manual rebuilding with Coot.[26] At the final stages of the refinement process, NCS restraints were removed from the protocol. Water molecules were added to the model near the end of the refinement by a search procedure based on peaks observed in the difference maps and bond distance criteria. Final structures satisfied the Molprobity criteria[27] at the corresponding resolutions. A summary of data collection and structure refinement statistics is shown in Table I.

Structural analysis

Contact distances between residues were analyzed using the program CONTACT from the CCP4 suite.[22]

Table I
Data Collection and Structure Refinement Statistics

Data collection		
Protein	TcTIM E104D	TbTIM E104D
Space group	P 1	P 1 21 1
Cell dimensions (Å)	$a = 38.72$, $b = 44.46$, $c = 69.04$ $\alpha = 95.02$, $\beta = 96.08$, $\gamma = 114.69$	$a = 88.09$, $b = 89.78$, $c = 181.72$ $\alpha = 90.00$, $\beta = 101.60$, $\gamma = 90.00$
Temperature (K)	100	100
Wavelength (Å)	0.9791	0.9791
Resolution limit (Å)	39.97–1.5	89.78–2.3
Reflection collected	136,044 (19,064)	368,306 (49,325)
Unique reflections[a]	63,005 (8958)	122,434 (17,590)
R_{merge}[b]	0.089 (0.25)	0.066 (0.264)
Mean $I/\sigma I$	5.7 (2.6)	8.1 (2.8)
Completeness (%)	95.6 (92.9)	99.6 (98.3)
Multiplicity	2.2 (2.2)	3.0 (2.8)
Wilson B-factor (Å^2)	14.19	36.51
Refinement		
R_{work}/R_{free} (%)[c]	16.71/19.63	20.71/26.14
No. atoms of protein/	3919/	22464/
Solvent/SO_4/glycerol/PEG	428/1/2/0	594/5/0/5
Average B-value (Å^2)	18.3	35.50
R.m.s.d. from ideal		
Bond lengths (Å^2)	0.008	0.009
Bond angles (°)	1.14	1.13
Ramachandran favored (%)	98.0	97.0
Ramachandran outliers (%)	0	0
PDB code	4HHP	4JEQ

[a]Values in parentheses correspond to the last resolution shell.
[b]$R_{merge} = \sum_j\sum_h(|I_{jh} - <I_h>|)/\sum_j\sum_h(<I_h>)$, where h is the unique reflection index, I_{jh} is the intensity of the symmetry-related reflection, and $<I_h>$ is the mean intensity.
[c]$R = \sum_h||F_o|_h - |F_c|_h|/\sum_h|F_o|_h$ for all reflections, where F_o and F_c are observed and calculated structure factors, respectively, and h defines unique reflections. R_{free} is calculated analogously for the test reflections, randomly selected, and excluded from refinement.

Structural analysis of the interfaces was performed using the PISA server,[28] and molecular graphic representations were drawn using PyMOL.[29]

Differential scanning calorimetry

DSC experiments were performed using a VP-DSC capillary calorimeter (GE Healthcare). Protein solutions were prepared by exhaustive dialysis against 100 m*M* TEA, 10 m*M* EDTA, and 1 m*M* DTT (pH 7.4). For experiments in the presence of urea, an adequate amount of a stock urea solution in the same buffer was added. Protein concentrations were determined from the absorbance at 280 nm, and urea concentrations were determined from refractive index measurements. Further details on the DSC experiments and the fitting of the calorimetric profiles with the two-state irreversible model can be found in previous publications.[30,31]

Calorimetric enthalpies for the irreversible thermal denaturation of the studied TIM proteins show significant variability, possibly reflecting differences in the irreversibly-denatured states. This, however, does not have any effect on the kinetic analysis of the DSC transitions, which ultimately depend only on the shape of the transitions. Note also that, when a defined value for the native to unfolded enthalpy change is needed (estimation of the unfolding and solvation-barrier contributions) we used the value predicted for TIM proteins by known structure-energetics relationships (see below).

RESULTS

Catalytic competence

After their expression in *E. coli*, the E104D TIM mutants of *T. cruzi*, *T. brucei*, *G. lamblia*, and *H. sapiens* were purified from extracts of the bacterial cells in which the enzymes were expressed. The properties of the enzymes were determined and compared to those of the respective wild types. The four mutants were catalytically competent, and, in relation to their respective wild types, there were no important differences in the kinetics of the conversion of glyceraldehyde-3-phosphate to dihydroacetone phosphate at various substrate concentrations (Table II).

Reactivation of the E104D mutants

It was previously reported[14] that the E104D mutation hinders the formation of active dimers of HsTIM from GdnHCl unfolded monomers. We explored this phenomenon in the wild type and mutants (Fig. 1). To this end,

Table II
Kinetic Constants of Wild-Type and Mutant E104D TIMs

TIM	V_{max} (μmol/min/mg)	K_m (m*M*)	k_{cat} (min^{-1})	k_{cat}/K_m (min^{-1} m*M*)
TcTIM	3581 ± 54	0.39 ± 0.03	$1.9 \times 10^5 \pm 2.5 \times 10^3$	$4.8 \times 10^5 \pm 4.0 \times 10^4$
TcTIM E104D	3913 ± 82	0.65 ± 0.11	$2.1 \times 10^5 \pm 4.5 \times 10^3$	$3.3 \times 10^5 \pm 5.0 \times 10^4$
TbTIM	3623 ± 485	0.38 ± 0.08	$1.9 \times 10^5 \pm 1.9 \times 10^4$	$5.2 \times 10^5 \pm 4.7 \times 10^4$
TbTIM E104D	3729 ± 439	0.69 ± 0.28	$1.9 \times 10^5 \pm 2.1 \times 10^4$	$2.9 \times 10^5 \pm 4.6 \times 10^4$
GlTIM	3188 ± 53	0.59 ± 0.06	$1.7 \times 10^5 \pm 3.0 \times 10^3$	$2.9 \times 10^5 \pm 3.3 \times 10^4$
GlTIM E104D	4167 ± 543	0.63 ± 0.09	$2.2 \times 10^5 \pm 2.9 \times 10^4$	$3.5 \times 10^5 \pm 5.7 \times 10^3$
HsTIM[a]	7080 ± 415	0.74 ± 0.10	$3.9 \times 10^5 \pm 5.2 \times 10^3$	$5.7 \times 10^5 \pm 8.7 \times 10^3$
HsTIM E104D[a]	6600 ± 354	0.70 ± 0.15	$3.7 \times 10^5 \pm 7.5 \times 10^3$	$5.2 \times 10^5 \pm 4.5 \times 10^3$

[a]From Rodriguez-Almazan *et al.*[14]

the enzymes and the E104D mutants were denatured in 6*M* GdnHCl; afterward, the mixture was diluted 100-fold and the appearance of activity was followed throughout time. In all the wild-type TIMs studied, dilution of the denaturant brought about the progressive appearance of activity, because, since TIM monomers are inactive,[9,10] the appearance of activity reflects association of the monomers. There were significant differences in the rate and extent of reactivation of the four wild types, which is in agreement with previous data on TcTIM and TbTIM.[10] The E104D mutants of the four TIMs also underwent reactivation, but it is relevant to note that the impact of the mutation was strikingly different in each of the four enzymes. The mutation induced rather small changes in the rate and extent of reactivation of TcTIM [Fig. 1(a)], whereas in the other TIMs, the mutation brought about significant decreases in the rate and extent at which the enzymes reactivated. In GlTIM, the effect was mainly on the extent of reactivation [Fig. 1(c)], whereas in TbTIM and HsTIM [Fig. 1(b,d), respectively], the effect was on both, the rate and extent of reactivation.

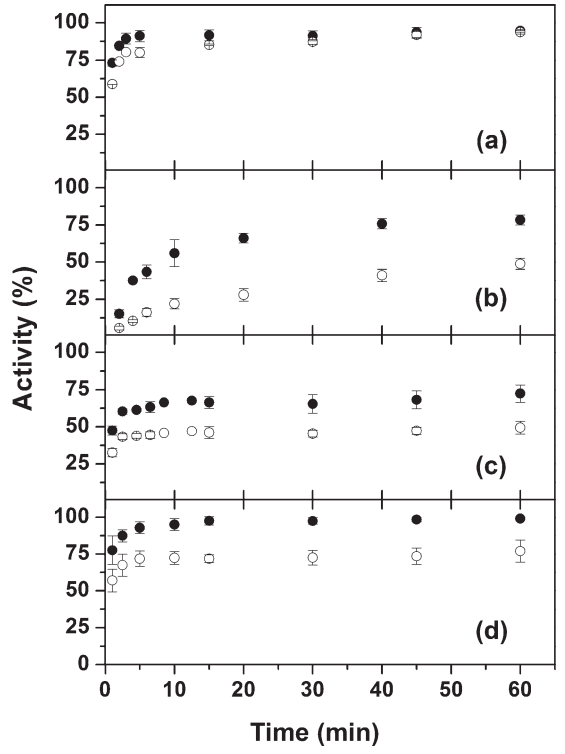

Figure 1
Reactivation of wild-type (closed symbols) and E104D mutants (open symbols) for TIM enzymes from *Trypanosoma cruzi* (**a**), *Trypanosoma brucei* (**b**), *Giardia lamblia* (**c**), and *Homo sapiens* (**d**).

Thermal denaturation

It has been reported that the incubation at 48°C of cell extracts of patients that have the E104D mutation[32,33] or that of recombinant E104D HsTIM[14] brings about a decrease in activity that is much more rapid than that of the controls. It is also relevant to point out that the thermal denaturation profile of TcTIM and TbTIM was previously studied by DSC.[30] Here, we extended the studies to HsTIM and GlTIM and the E104D mutants of the four enzymes. In all cases, the calorimetric transitions were irreversible as indicated by the lack of thermal effect in reheating runs; however, the transitions were strongly dependent on the scanning rate (Figs. 2 and 3), implying that the denaturation process is under kinetic control. The calorimetric traces are adequately described by the two-state irreversible model,[30,34] whereupon heating, the native protein (N) undergoes a transition to a final state (F) unable to fold back to the native state. The kinetic conversion between these two states ($N \rightarrow F$) is described by a first-order rate constant that changes with temperature according to the Arrhenius equation. The fits of this model to the heat capacity profiles were excellent (Figs. 2 and 3). The compliance of these profiles with the model indicates that the kinetically relevant transition state is dimeric, which is consistent with the fact that we did not observe a significant effect of protein concentration on the calorimetric transitions (the maximum of DSC transitions, T_m, shifted only one degree on going from a protein concentration of 0.4–2 mg/mL, data not shown).

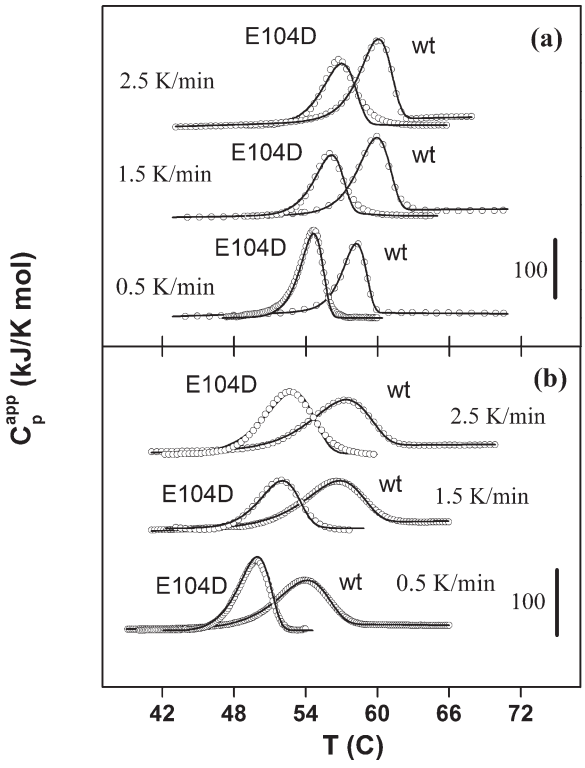

Figure 2

Illustrative examples of experimental DSC thermograms for TcTIM and its E014D mutant (**a**) and for TbTIM and its E104D mutant (**b**) at the indicated scan rates. The thermograms for wild-type TcTIM and TbTIM are from Costas *et al.*[30] The profiles at other scan rates were qualitatively similar. Symbols represent experimental apparent heat capacity data, and continuous lines are the best fits of the two-state irreversible model. Note that, for clarity, the profiles have been shifted in the *y*-axis.

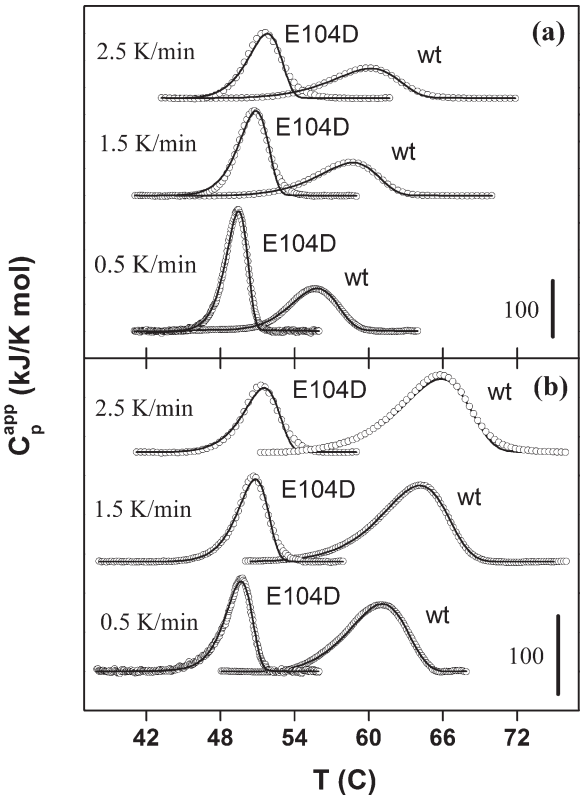

Figure 3

Illustrative examples of experimental DSC thermograms for GlTIM and its E014D mutant (**a**) and for HsTIM and its E104D mutant (**b**) at the indicated scan rates. The profiles at other scan rates were qualitatively similar. Symbols represent experimental apparent heat capacity data, and continuous lines are the best fits of the two-state irreversible model. Note that, for clarity, the profiles have been shifted in the *y*-axis.

The activation energies (E_A) for thermal denaturation of the four enzymes and their mutants as obtained from the Arrhenius plots (Fig. 4) are reported in Table III. There is a huge range of E_A values amongst the wild-type proteins (from ~350 to 800 kJ mol^{-1}) and also between the four E104D mutants (from around 480 to nearly 800 kJ mol^{-1}). On comparing E_A for a given wild-type TIM with the corresponding value for its E104D mutant, it is observed that the mutation affects the activation energy for thermal denaturation to markedly different extents; for example in HsTIM the mutation increased the activation energy by about 430 kJ mol^{-1}, whereas in TcTIM, the mutation decreased it by 78 kJ mol^{-1}. Clearly in different TIMs the conservative E104D mutation induces

Table III

Activation Energies E_A (kJ mol^{-1}), First-Order Rate Constant k (min^{-1}) at 37°C, Kinetic Urea m (kJ mol^{-1} M^{-1}) Value ($m^{\neq}$), Urea m (kJ mol^{-1} M^{-1}) Value for Equilibrium Unfolding (m_{EQ}), Fractional Degrees of Exposure to the Solvent (~Fractional Degrees of Unfolding) in the Transition States ($m^{\neq}/m_{EQ}$) for Wild-Type and Mutant E104D TIMs

	TcTIM[a]	TcTIM E104D	TbTIM[a]	TbTIM E104D	GlTIM	GlTIM E104D	HsTIM	HsTIM E104D
E_A	792.8 ± 17.6	714.7 ± 14.6	397.9 ± 4.6	480.6 ± 11.0	366.6 ± 7.0	647.0 ± 20.3	361.2 ± 3.8	795.5 ± 20.7
k	1.1 × 10^{-9}	1.2 × 10^{-7}	6.7 × 10^{-5}	1.6 × 10^{-4}	5.8 × 10^{-5}	2.4 × 10^{-5}	7.2 × 10^{-6}	3.2 × 10^{-6}
$m^{\neq}$	8.34 ± 0.12	9.48 ± 0.15	1.69 ± 0.20	4.23 ± 0.22	3.94 ± 0.44	11.00 ± 0.12	2.77 ± 0.05	13.55 ± 0.62
m_{EQ}[b]	30.67	30.67	30.35	30.35	30.02	30.02	30.09	30.09
$m^{\neq}/m_{EQ}$	0.272 ± 0.01	0.309 ± 0.01	0.056 ± 0.008	0.140 ± 0.01	0.131 ± 0.02	0.367 ± 0.01	0.092 ± 0.002	0.451 ± 0.05

[a]From Costas *et al.*[30]

[b]Calculated using the correlation presented by Myers *et al.*[35] The necessary accessible surface areas were calculated from the Protein Data Bank files and a modification of the Shrake–Rupley algorithm as described in Costas *et al.*[30]

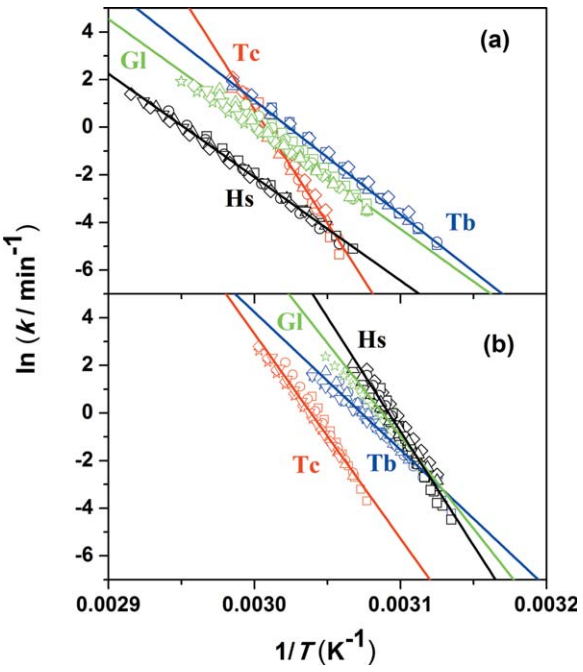

Figure 4

Arrhenius plots for the irreversible thermal denaturation of the wild-type TIMs (**a**) and their E104D mutants (**b**). Data for wild-type TcTIM and TbTIM are from Costas *et al.*[30] The protein concentrations were 0.4 mg mL^{-1}. The different symbols correspond to the different scan rates used in the DSC experiments (0.5, 1, 1.5, 2, 2.5, and 3 K min^{-1}). The lines are the best fits of the Arrhenius equation $k = \exp[(-E_A/R)(1/T - 1/T^*)]$. The values of the activation energies E_A are given in Table III.

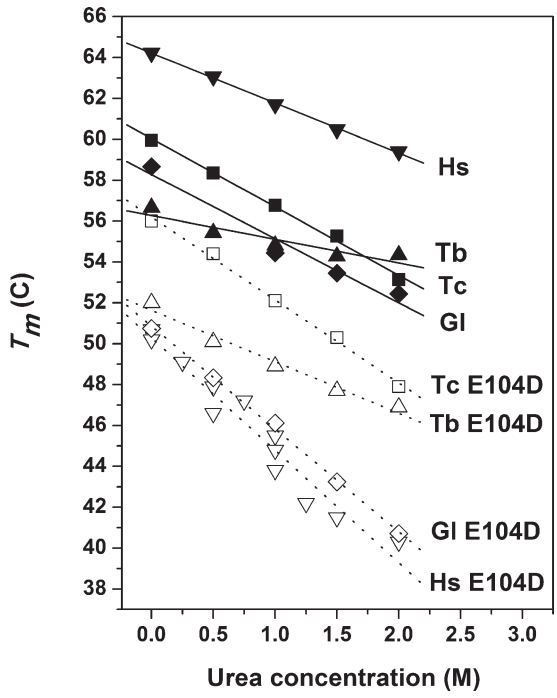

Figure 5

The effect of urea concentration on the temperature of the maximum of DSC transitions (T_m) for the TIM proteins studied in this work. Data for wild-type TcTIM and TbTIM are from Costas *et al.*[30] The lines are the best fits of straight lines to the data (symbols). The protein concentrations were 0.4 mg mL^{-1}. The T_m values shown correspond to a scan rate of 1.5 K min^{-1}, although T_m values obtained at other scanning rates give very similar dependencies and, in particular, give essentially the same values for the slope $dT_m/d[\text{urea}]$.

significantly different alterations in the energetics of the transition state during thermal denaturation.

Kinetic stability and transition state plasticity

The different activation energies of the TIMs studied may contribute to different rates of denaturation at the temperature in which the organism lives. Thus, it was considered relevant to compare the kinetic stability of the four enzymes and the mutants at the same temperature, that is, 37°C. To this end, we made a rather short Arrhenius extrapolation to 37°C of the data in Figure 4; the k values at 37°C for the various TIMs are given in Table III. For TcTIM and TcTIM E104D, the values were several orders of magnitude slower than those of the other proteins, indicating that kinetic stability of the two former TIMs is much higher than that of the other enzymes.

We also examined if the differences in thermal unfolding of the proteins, and their respective mutants, are related to their solvent accessible surfaces. The denaturant concentration effects on free energy changes and the corresponding changes in solvent accessible surface have been well documented[35] and are represented by the so-called m values. The kinetic urea values $m^{\neq} = -\delta\Delta G^{\neq}/\delta[\text{urea}]$ are conveniently derived from the urea concentration dependence of the maximum of DSC transitions (T_m) and the activation energy using[31]:

$$m^{\neq} = -\frac{E_A}{T_m}\left(\frac{dT_m}{d[\text{urea}]}\right) - RT_m\left(\frac{d\ln\left(E_A/RT_m^2\right)}{d[\text{urea}]}\right) \qquad (1)$$

since the derivatives involved are readily available. The second term in Eq. (1) is small (accounts for a maximum of 15% of the total $m^{\neq}$ value for the proteins studied here), therefore the $m^{\neq}$ values (Table III) are mainly given by $dT_m/d[\text{urea}]$ which can be accurately determined from the experimental urea dependence of the T_m values shown in Figure 5. The kinetic $m^{\neq}$ values can be transformed into fractional degrees of unfolding (exposure to solvent) in the transition state by calculating the ratio $m^{\neq}/m_{EQ}$, where m_{EQ} is an urea-value for equilibrium unfolding devoid from strong distortions caused by residual structure in the unfolded state; to estimate these m_{EQ} values, we have therefore resorted to the general correlation reported by Myers *et al.*[35] The $m^{\neq}/m_{EQ}$

ratios (Table III) are larger for the E104D mutants than for the corresponding wild-type TIMs, indicating a greater exposure to solvent in the transition state for the mutants. It is noteworthy that there are marked differences between the four enzymes: in HsTIM, for example, the mutation brought about a fivefold increase, whereas in TcTIM the mutation increased the $m^{\neq}/m_{EQ}$ ratio 1.1 times. Figure 6 shows that the effect of the E104D mutation on denaturation temperature, $\Delta T_m = T_m(E104D) - T_m(wt)$, is clearly correlated with its effect on the exposure to solvent of the transition state, $\Delta(m^{\neq}/m_{EQ}) = m^{\neq}/m_{EQ}(E104D) - m^{\neq}/m_{EQ}(wt)$. Therefore, the deleterious effect of this apparently very conservative mutation is linked to the kinetic stability and transition-state plasticity of the proteins.

Activation, unfolding, and solvation-barrier contributions

As shown before,[30] the experimental activation energies in Table III cannot be solely explained in terms of the degree of unfolding in the transition states. Instead, it is necessary to invoke an additional energetic contribution, which is absent in the native states; this has been termed solvation-barrier contribution, since it is associated with partially broken, water-unsatisfied interactions in the transition states. To estimate the impact of the E104D mutation in the activation, unfolding, and solvation-barrier contributions, as well as in the enthalpic, entropic, and free energy components of the process, we used the calculation scheme described below which follows the general lines of our previously published work.[30] This analysis uses 335.15 K (60°C) as a reference temperature. This is convenient because 60°C is roughly in the middle of the denaturation temperature range defined by the proteins studied in this work and also because it is the reference temperature used by Robertson *et al.*[36] in their structural parametrization of protein energetics.

The activation energies E_A (or enthalpies since $E_A \cong \Delta H^{\neq}$ at atmospheric pressure) at the corresponding T_m values can be calculated at a reference temperature T_0 (333.15 K) using

$$\Delta H^{\neq}(T_0) = E_A + \Delta C_P^{\neq} \cdot (T_0 - T_m) \quad (2)$$

Assuming that the activation heat capacity ($\Delta C_P^{\neq}$) is equal to total heat capacity scaled by the accessibility (the degree of exposure to the solvent in the transition state ($m^{\neq}/m_{EQ}$)), and that there is no solvation-barrier contribution ($\Delta C_P^{*} = 0$),

$$\Delta C_P^{\neq} = \Delta C_{P,EQ} \cdot \left(\frac{m^{\neq}}{m_{EQ}}\right) \quad (3)$$

where $\Delta C_{P,EQ}$ is the heat capacity change upon equilibrium unfolding that can be estimated using the well known correlation between the unfolding enthalpy and the number of residues in the protein[36] (this correlation also uses 333.15 K as the reference temperature). The result using TIM proteins is that $\Delta C_{P,EQ} = 28.35$ kJ/K mol, but the conclusions reached (see below) using $\Delta C_{P,EQ} = 0$ or 56.7 kJ/K mol are qualitatively the same. From Eq. (3), the activation enthalpies at T_0 are given by

$$\Delta H^{\neq}(T_0) = E_{act} + \Delta C_{P,EQ} \cdot \left(\frac{m^{\neq}}{m_{EQ}}\right)(T_0 - T_m) \quad (4)$$

In the transition-state theory, the relation between the rate constant k for unfolding/denaturation and the activation thermodynamic parameters is

$$k = k_0 \exp\left(-\frac{\Delta G^{\neq}}{RT}\right) \quad (5)$$

$$\Delta G^{\neq} = \Delta H^{\neq} - T\Delta S^{\neq} \quad (6)$$

Using these two equations, the activation entropy at the T_m is given as

$$\Delta S^{\neq}(T_m) = \frac{\Delta H^{\neq}(T_m)}{T_m} - \frac{\Delta G^{\neq}(T_m)}{T_m} = \frac{E_{act}}{T_m} + R\ln k_m - R\ln k_0 \quad (7)$$

and since at the reference temperature T_0,

$$\Delta S^{\neq}(T_0) = \Delta S^{\neq}(T_m) + \Delta C_P^{\neq} \cdot \ln\left(\frac{T_0}{T_m}\right) \quad (8)$$

the activation entropy at T_0 is given by:

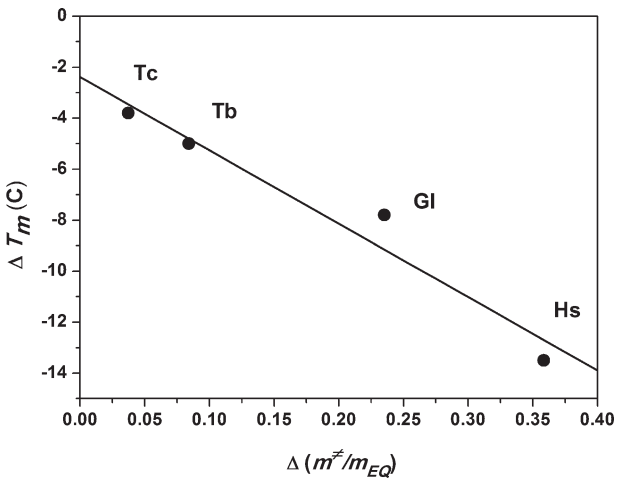

Figure 6

The effect of the E104D mutation. Correlation between the change on denaturation temperature [$\Delta T_m = T_m(E104D) - T_m(wt)$] and the change of exposure to solvent of the transition state [$\Delta(m^{\neq}/m_{EQ}) = m^{\neq}/m_{EQ}(E104D) - m^{\neq}/m_{EQ}(wt)$] for the TIM proteins studied in this work. ΔT_m was calculated from the T_m values obtained from the DSC scans at 1.5 K min^{-1}.

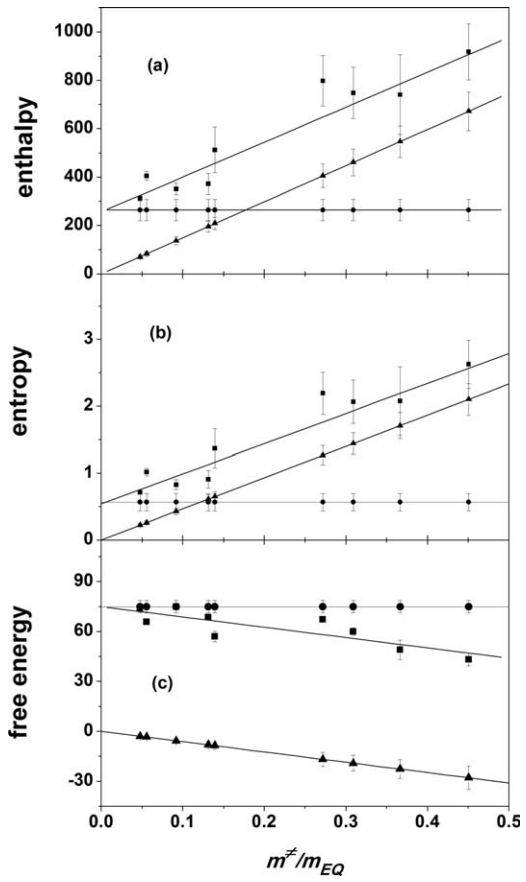

Figure 7

Activation (■), solvation (●), and unfolding (▲) contributions to the enthalpy (**a**), entropy (**b**), and free energy (**c**) against the fractional degree of unfolding (exposure to the solvent) in the transition state, $m^{\neq}/m_{EQ}$, for the TIM proteins studied in this work, according to Eqs. (11–13). Data for the TIM of *Leishmania mexicana* from Costas *et al.*[30] were also included. The lines are the best fits of straight lines to the data. The units for the enthalpy and free energy are kJ mol^{-1} and for the entropy kJ K^{-1} mol^{-1}, respectively.

$$\Delta S^{\neq}(T_0) = \frac{E_{act}}{T_m} + R\ln k_m - R\ln k_0 + \Delta C_{P,EQ}\left(\frac{m^{\neq}}{m_{EQ}}\right)\ln\left(\frac{T_0}{T_m}\right) \quad (9)$$

where $Rlnk_0 = 0.207$ kJ/K mol has been previously estimated.[30] The activation free energy at T_0 is immediately obtained using:

$$\Delta G^{\neq}(T_0) = \Delta H^{\neq}(T_0) - T_0\Delta S^{\neq}(T_0) \quad (10)$$

To obtain the unfolding and solvation contributions at T_0, we make two additional assumptions. The first is that in the transition state, the unfolding contributions (ΔX_{unf}) scale with accessibility with a coefficient equal to the change associated with total unfolding. The second is that the solvation contributions (ΔX^*) are constant and equal for the wild-type TIMs and their E104D mutants. Hence,

$$\Delta H^{\neq} = \Delta H^* + \Delta H_{unf} = \Delta H^* + \Delta H_{EQ}\cdot\left(\frac{m^{\neq}}{m_{EQ}}\right) \quad (11)$$

$$\Delta S^{\neq} = \Delta S^* + \Delta S_{unf} = \Delta S^* + \Delta S_{EQ}\cdot\left(\frac{m^{\neq}}{m_{EQ}}\right) \quad (12)$$

$$\Delta G^{\neq} = \Delta G^* + \Delta G_{unf} = \Delta G^* + \Delta G_{EQ}\cdot\left(\frac{m^{\neq}}{m_{EQ}}\right) \quad (13)$$

Therefore, plots of $\Delta X^{\neq}$ against $m^{\neq}/m_{EQ}$ provide both the unfolding and solvation-barrier contributions. Figure 7 shows that in fact $\Delta X^{\neq}$ varies linearly with accessibility (correlation coefficients raging from 0.96 to 0.84) and displays the ΔX^* and ΔX_{unf} contributions.

The effect of the E104D mutation in the enthalpic, entropic and free energy components of the activation and unfolding contributions (those for solvation are null, under the assumptions noted above) can be obtained as $\Delta\Delta X = \Delta X(\text{E104D}) - \Delta X(\text{wt})$ and are shown in Figure 8 as a function of the accessibility change upon mutation, $\Delta(m^{\neq}/m_{EQ}) = m^{\neq}/m_{EQ}(\text{E104D}) - m^{\neq}/m_{EQ}(\text{wt})$. Figure 9 shows that $\Delta\Delta G^{\neq}$ and $\Delta\Delta G_{unf}$ clearly correlate with the effect of the E104D mutation on the maximum of the DSC transitions, ΔT_m. This indicates that the decrease in thermal stability (as measured by ΔT_m) correlates with an increase in the fractional degree of exposure to the solvent in the transition state (Fig. 6) which, in turn, is reflected in the activation and unfolding free energy barriers (Fig. 9) for the irreversible denaturation, that ultimately determine the protein kinetic stability. As seen in Figure 9, these effects are small for TcTIM but quite large for HsTIM.

Structure of wild type and mutants in the vicinity of Glu104

In an attempt to understand the different impact that the E104D mutation has on the TIMs we studied, we crystallized and solved the structure of the E104D mutants of TbTIM and TcTIM; the crystal structure of E104D HsTIM has been described[14] and we were unable to crystallize the E104DGlTIM mutant. The structures were compared with the reported structures of their respective wild types. A notable feature in the structures of the wild-type and the mutant enzymes is that their overall structures superpose quite well, as shown by the RMSD deviation between the C_α of wild-type and mutant enzymes (Supporting Information Figure S1). Accordingly, we focused on the region of residue 104 in the wild-type and mutant enzymes. As shown in Figure 10, Glu104 is part of a conserved cluster of five residues in each monomer. In the four wild-type enzymes, the geometry between these residues is largely conserved, the distance between Glu104 of the two subunits being in a similar range. Figure 10 also shows the arrangement of

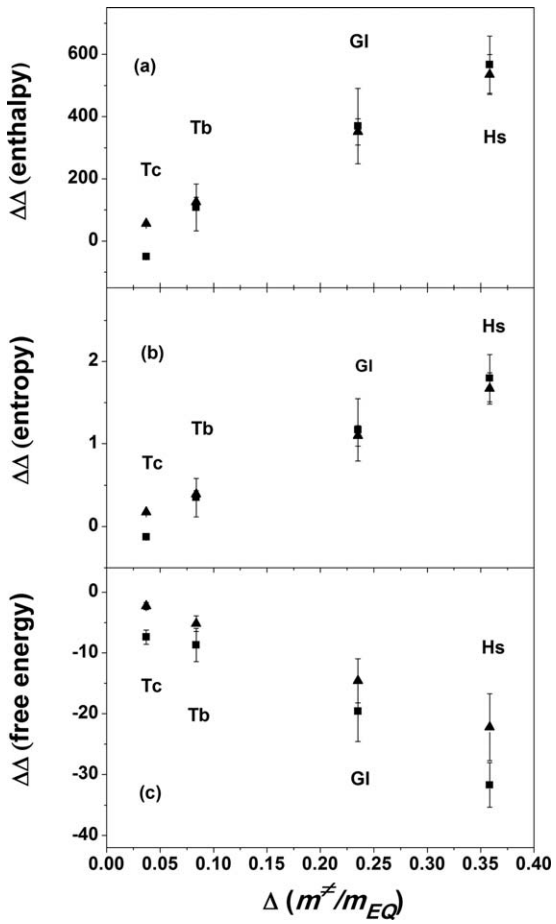

Figure 8

The effect of the E104D mutation [$\Delta\Delta X = \Delta X(\text{E104D}) - \Delta X(\text{wt})$] on the activation (■) and unfolding (▲) enthalpy (**a**), entropy (**b**), and free energy (**c**) against the change of exposure to solvent of the transition state, [$\Delta(m^{\neq}/m_{EQ}) = m^{\neq}/m_{EQ}(\text{E104D}) - m^{\neq}/m_{EQ}(\text{wt})$], for the TIM proteins studied in this work. Units for the enthalpy and free energy are kJ mol^{-1} and for the entropy kJ K^{-1} mol^{-1}, respectively.

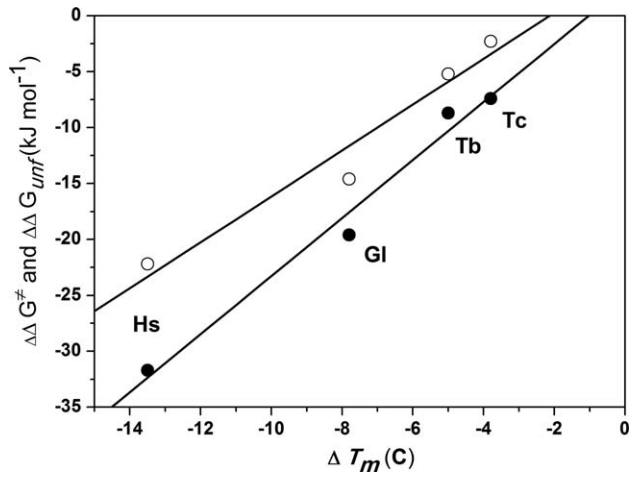

Figure 9

The effect of the E104D mutation. Correlation between the change on activation (filled symbols) and unfolding (open symbols) free energy and the change on denaturation temperature, ΔT_m, for the TIM proteins studied in this work. ΔT_m was calculated from the T_m values obtained from the DSC scans at 1.5 K min^{-1}

these residues in the E104D mutants of HsTIM, TbTIM, and TcTIM. The data show that there are no important and consistent differences between the wild-type and mutant enzymes, except that the intermonomeric salt bridge between Glu77 and Arg 98 is missing in the HsTIM mutant, while it is conserved in both TbTIM and TcTIM. Also, the distance between residues 104 of the two subunits is larger in the case of the mutant enzymes.

As there are no obvious differences that could account for the effect of the E104D mutation, we examined the residues that are in the first shell of Glu104, at a cut off distance of 4 Å, as well as those present in the second shell (Supporting Information Tables S1 and S2). For the latter, we centered on the corresponding residue of the first shell and identified those residues that are at a distance of <4 Å. We found no significant differences for Glu104 when the residues of the first shell of the wild-type enzymes were compared with those of the mutant enzymes. Likewise, both, the wild-type and mutant enzymes have the same, or equivalent, residues in the second shell and at markedly similar distances. It is appropriate to note that wild-type GlTIM exhibits the same basic structure in the vicinity of Glu104. However, GlTIM differs from the other enzymes in the residues that are in the second shell; this is due to differences in its amino acid sequence and not to alterations of its general structure.

Taken together, the data from the crystal structures of the wild-type and mutant enzymes show that the different impacts of the E104D mutation on the four enzymes that were studied, are not due to differences in the molecular environment of Glu104, but that, most likely, the differences result from the molecular context in which the E104D mutation is introduced.

DISCUSSION

It has been reported that mutations of nonconserved amino acids may not affect function, especially if they are on the surface of the enzyme; however, function is affected,[37] if the mutations are combined with other mutations that *per se* have no functional influence. It is also well known that the detrimental effect of a mutation may be compensated by introduction of additional mutations[38–40]; in fact, the analysis of amino acid sequences often reveals that during evolution, the replacement of an amino acid that is important for function is accompanied by covariations of other residues.[41] Thus, it is logical to assume that in evolution, whenever an amino acid is changed, its function will either be abolished or

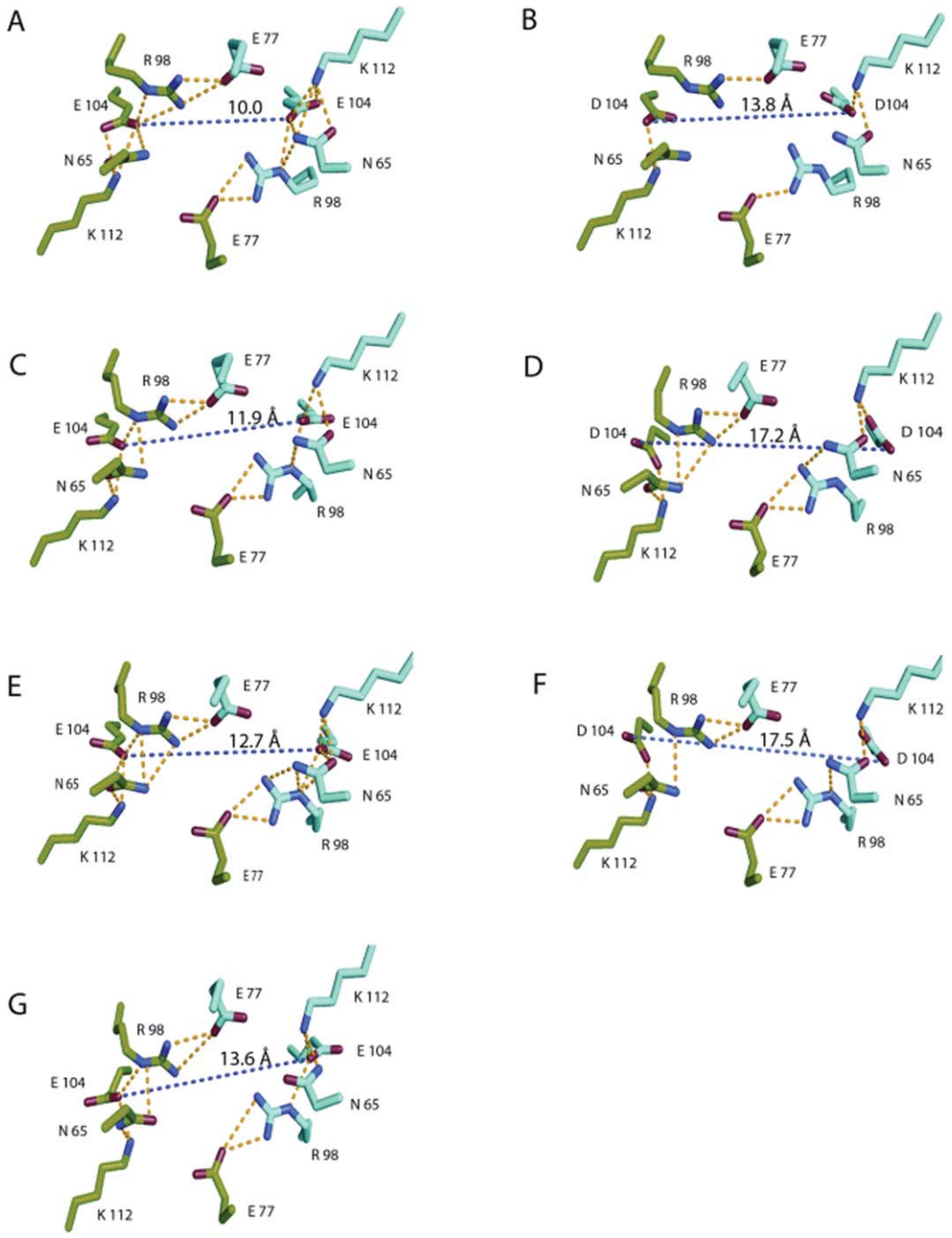

Figure 10

Conserved cluster of five residues in the interface region in the wild-type and mutant enzymes. The cluster is formed by Asn 65, Glu 77, Arg 98, Glu 104, and Lys 112 for each subunit (monomer A in green and monomer B in cyan). The seven panels are: (**A**) HsTIM wt (PDB code: 2JK2), (**B**) HsTIM E104D (PDB code: 2VOM), (**C**) TcTIM wt (PDB code: 1TCD), (**D**) TcTIM E104D (PDB code: 4HHP), (**E**) TbTIM wt (PDB code: 2J27), (**F**) TbTIM E104D (PDB code: 4JEQ), and (**G**) GlTIM wt (PDB code: 4BI7). The distances between residues 104 were estimated using the atoms OE2 and OD2 of glutamate and aspartate, respectively. The yellow dots depict atoms that are closer than 3.5 Å. Other than the salt bridge between Glu77 (monomer A) and Arg 98 (monomer B), there are no residues of the other subunit at <4 Å.

preserved depending on the adequacy of the interactions that may be established. In this regard, it is relevant to point out that the properties of an amino acid within a protein structure can be modulated by its contacts with neighboring residues, but also by distant residues. An example of the latter phenomena is illustrated in TIM. The enzymes from some parasites have an interface Cys surrounded by residues of loop3 of the other subunit. It has been reported that chemical derivatization (thiomethylation) of the Cys induces strikingly different effects

in different TIMs.[20,42] It was shown that the impact of derivatization is related to the dimensions of loop3, the larger the loop the lower the detrimental effect of derivatization. Likewise, it was reported[3] that the reactivity of the Cys depends on the existence of particular amino acids that are far from the interface Cys. Collectively, the data illustrate that in proteins, amino acids may be replaced or undergo chemical alterations without loss of function, provided that the local environment and/or the network of interactions of distant residues confers resistance to the perturbing agent.

Therefore, it may be asked if amino acids that exist in all sequences of homologous enzymes have been conserved because the system does not tolerate a change of such residue, even if the mutation is conservative. In the case of catalytic residues, the answer seems quite obvious, catalysis requires the participation of residues with strict chemical and physicochemical properties that have to be positioned at precise geometrical distances; hence, it is very difficult to find a replacement. In this context, it is noteworthy that Saab-Rincón *et al.*[43] were able to confer to TIM the capacity to express thiamine phosphate synthase activity. On the other hand, there are residues, such as Glu104 of TIM, that do not directly participate in catalysis, and yet they are present in all homologous enzymes. *A priori*, it may be assumed that these residues are essential for folding or for maintaining protein stability. Indeed, in the TIMs that were here examined, we observed that the E104D mutation affects dimer formation and the kinetic stability of TIMs from four different organisms. However, there were striking differences in the susceptibility of the enzymes to the E104D mutation, indicating that in enzymes that carry out the same function, even if they have high sequence identity, conserved amino acids do not contribute to the same extent to the global properties of homologous enzymes.

The latter findings indicate that the functional importance of an amino acid, even if it is conserved, depends on the rest of the protein and raise the question of how the contribution of conserved amino acids to the general properties of a protein should be evaluated. This is a difficult problem since each homologous enzyme has a particular amino acid sequence, and hence different amino acid interactions. Indeed, the diversity in amino acid sequences may explain why TIMs from different organisms in which the same $(\alpha/\beta)_8$ structure was built with different amino acids exhibit different susceptibilities to the E104D mutation. In addition, and because homologous enzymes have different amino acid composition, it may be speculated that enzymes acquired their particular structural features as an adaptation to the demands of the environments in which the cells live. For example, *T. cruzi* and *T. brucei* have a complex life cycle[44]; they thrive in intra- and extracellular media as well in two markedly different hosts (mammals and triatominae or flies of the genus glossina, respectively). Throughout their lives, these parasites successfully resist marked changes in pH, temperature, oxygen concentration, and ion composition. In comparison to the life cycle of trypanosomes, that of *G. lamblia* is relatively simple[44]; these parasites live in mammalian intestinal tracts until they are excreted and acquire the cystic form that can again be ingested by mammal. In contrast to the parasites, the cells of *H. sapiens* subsist in rather constant conditions. Thus, it may be more than a coincidence that the magnitude of the E104D induced changes in the denaturation temperature T_m and the exposure to solvent in the transition state of the four enzymes follow the sequence TcTIM < TbTIM < GlTIM < HsTIM (see Figs. 6 and 9). In particular, it is noteworthy that the kinetic stability of the protein depends on the previous mutational background, suggesting that kinetic stability might be an important feature of epistasis.[45,46] Of course, it is clear that the possible relation between the kinetic stability of enzymes and the life conditions of the organisms deserves further studies. Nonetheless, the overall data of this work illustrate that because each homologous enzyme has a particular sequence and a distinctive set of amino acid interactions, it should be regarded as a unique entity that has evolved for function and stability in the organisms to which it belongs.

ACKNOWLEDGMENTS

The authors thank Dr. Pavel Afonine for his help in the crystal structures refinements. They also thank Dr. Georgina Garza-Ramos for her useful comments to this work.

REFERENCES

1. Minor DL, Kim PS. Context-dependent secondary structure formation of a designed protein sequence. Nature 1996;380:730–734.
2. Lockless SW, Ranganathan R. Evolutionary conserved pathways of energetic connectivity in protein families. Science 1999;286:295–299.
3. García-Torres I, Cabrera N, Torres-Larios A, Rodríguez-Bolaños M, Díaz-Mazariegos S, Gómez-Puyou A, Pérez-Montfort R. Identification of amino acids that account for long-range interactions in two triosephosphate isomerases from pathogenic trypanosomes. PLoS One 2011;6:e1879.
4. Freire E. The propagation of binding interactions to remote sites in proteins: and analysis of the monoclonal antibody D1.3 to lysozyme. Proc Natl Acad Sci USA 1999;96:10118–10122.
5. Halabi N, Rivoire O, Leibler S, Rangantahan R. Protein sectors: evolutionary units of three-dimensional structure. Cell 2009;138:774–786.
6. Hey Y, Chen Y, Alexander P, Bryan PN, Orban J. NMR structure of two designed proteins with high sequence similarity, but different folds and function. Proc Natl Acad Sci USA 2008;105:14412–14417.
7. Knowles JR. Enzyme catalysis: not different, just better. Nature 1991;350:121–124.
8. Wierenga RK, Kapetaniou EG, Venkatesan R. Triosephosphate isomerase: a highly evolved biocatalyst. Cell Mol Life Sci 2010;67:3961–3982.

9. Waley SG. Refolding of triose phosphate isomerase. Biochem J 1973;135:165–172.
10. Zomosa-Signoret V, Hernández-Alcántara G, Reyes-Vivas H, Martínez-Martínez E, Garza-Ramos G, Pérez-Montfort R, Tuena de Gómez-Puyou M, Gómez-Puyou A. Control of reactivation kinetics of homodimeric triosephosphate isomerase from unfolded monomers. Biochemistry 2003;42:3311–3318.
11. Schneider AS. Triosephosphate isomerase deficiency: historical perspectives and molecular aspects. Baillieres Best Pract Res Clin Haematol 2000;13:119–140.
12. Orosz F, Oláh J, Ovadi J. Triosephosphate isomerase deficiency facts and doubts. IUBMB Life 2006;58:703–715.
13. Orosz F, Oláh J, Ovadi, J. Triosephosphate isomerase deficiency: new insights into an enigmatic disease. Biochim Biophys Acta 2009; 1792:1168–1174.
14. Rodríguez-Almazán C, Arreola R, Rodríguez-Larrea D, Aguirre-López B, Tuena de Gómez-Puyou M, Pérez-Montfort R, Costas M, Gómez-Puyou A, Torres-Larios A. Structural basis of triosephosphate isomerase deficiency: mutation E104D is related to alterations of a conserved water network at the dimer interface. J Biol Chem 2008;283:23254–23263.
15. Wierenga RK, Noble MEM, Vriend G, Nauche S, Hol WGJ. Refined 1.83 Å of trypanosomal triosephosphate isomerase crystallized in the presence of 2.4 M ammonium sulphate. A comparison with the structure of the trypanosomal triosephosphate isomerase-glycerol-3-phosphate complex. J Mol Biol 1991;220:995–1015.
16. Maldonado E, Soriano-García M, Moreno A, Cabrera N, Garza-Ramos G, Tuena de Gómez-Puyou M, Gómez-Puyou A, Pérez-Montfort R. Differences in the intersubunit contacts in triosephosphate isomerase from two closely related pathogenic trypanosomes. J Mol Biol 1998;283:193–203.
17. Reyes-Vivas H, Díaz A, Peón J, Mendoza-Hernández G, Hernández-Alcántara G, de la Mora-de la Mora I, Enriquez-Flores S, Domínguez-Ramírez L, López-Velarde G. Disulfide bridges in the mesophilic triosephosphate isomerase from *Giardia lamblia* are related to oligomerization and activity. J Mol Biol 2007;365:752–763.
18. Borchert TV, Pratt K, Zeelen JP, Callens M, Noble ME, Opperdoes FR, Michels PA, Wierenga RK. Overexpression of trypanosomal triosephosphate isomerase in *Escherichia coli* and characterisation of a dimer-interface mutant. Eur J Biochem 1993;211:703–710.
19. Ostoa-Saloma P, Garza-Ramos G, Ramírez J, Becker I, Berzunza M, Landa A, Gómez-Puyou A, Tuena de Gómez-Puyou M, Pérez-Montfort R. Cloning, expression, purification and characterization of triosephosphate isomerase from *Trypanosoma cruzi*. Eur J Biochem 1997;244:700–705.
20. Enriquez-Flores S, Rodríguez-Romero A, Hernández-Alcántara G, Oria-Hernández J, Gutiérrez-Castrellón P, Pérez-Hernández G, de la Mora de la Mora I, Castillo-Villanueva A, García-Torres I, Mendez ST, Gómez-Manzo S, Torres-Arroyo A, López-Velazquez G, Reyes-Vivas H. Determining the molecular mechanism of inactivation by chemical modification of triosephosphate isomerase from the human parasite *Giardia lamblia*: a study for antiparasitic drug design. Proteins 2011;79:2711–2724.
21. Kabsch W. XDS. Acta Crystallogr D Biol Crystallogr 2010;66:125–132.
22. Collaborative Computational Project, Number 4. The CCP4 suite: programs for protein crystallography. Acta Crystallogr D Biol Crystallogr 1994;50:760–763.
23. Evans P. Scaling and assessment of data quality. Acta Crystallogr D Biol Crystallogr 2006;62:72–82.
24. McCoy AJ, Grosse-Kunstleve RW, Adams PD, Winn MD, Storoni LC, Read RJ. Phaser crystallographic software. J Appl Crystallogr 2007;40:658–674.
25. Adams PD, Afonine PV, Bunkoczi G, Chen VB, Davis IW, Echols N, Headd JJ, Hung LW, Kapral GJ, Grosse-Kunstleve RW, McCoy AJ, Moriarty NW, Oeffner R, Read RJ, Richardson DC, Richardson JS, Terwilliger TC, Zwart PH. PHENIX: a comprehensive Python-based system for macromolecular structure solution. Acta crystallogr D, Biol crystallogr 2010;66, 213–221.
26. Emsley P, Lohkamp B, Scott WG, Cowtan K. Features and development of Coot. Acta Crystallogr D Biol Crystallogr 2010;66:486-501.
27. Chen VB, Arendall WB, III, Headd JJ, Keedy DA, Immormino RM, Kapral GJ, Murray LW, Richardson JS, Richardson DC. MolProbity: all-atom structure validation for macromolecular crystallography. Acta Crystallogr D Biol Crystallogr 2010;66:12–21.
28. Krissinel E, Henrick KJ. Inference of macromolecular assemblies from crystalline state. J Mol Biol 2007;372:774–797.
29. DeLano WL. The PyMOL molecular graphics system. San Carlos, CA: DeLano Scientific, 2002.
30. Costas M, Rodríguez-Larrea D, de Maria L, Borchert T, Gómez-Puyou A, Sánchez-Ruiz JM. Between species variation in the kinetic stability of TIM proteins linked to solvation-barrier free energies. J Mol Biol 2009;385:924–937.
31. Rodríguez-Larrea D, Minning S, Borchert TV, Sanchez-Ruiz JM. Role of solvation barriers in protein kinetic stability. J Mol Biol 2006;360:715–724.
32. Daar IO, Artymiuk PJ, Phillips DC, Maquat LE. Human triosephosphate isomerase deficiency: a single amino acid subsitution results in a thermolabile enzyme. Proc Natl Acad Sci USA 1986;83: 7903–7907.
33. Repiso A, Boren J, Ortega F, Pujades A, Centelles J, Vives-Corrons JL, Climent F, Cascante M, Carreras J. Triosephosphate isomerase deficiency: genetic, enzymatic and metabolic characterization of a new case from Spain. Haematologica 2002;87:ECR12.
34. Sánchez-Ruíz JM. Theoretical analysis of the Lumry-Eyring models in differential scanning calorimetry. Biophys J 1992;61:921–935.
35. Myers JK, Pace CN, Scholtz JM. Denaturant *m* values and heat capacity changes in accessible surface areas of protein folding. Protein Sci 1995;4:2138–2148.
36. Robertson AD, Murphy KP. Protein structure and the energetics of protein stability. Chem Rev 1997;97:1251–1268.
37. Axe DD. Extreme functional sensitivity in conservative amino acid changes on enzyme exteriors. J Mol Biol 2000;301:585–596.
38. Yanofsky C, Horn V, Thorpe D. Protein structure relationships revealed by mutational analysis. Science 1964;146:1593–1594.
39. Davis BH, Poon AFY, Whitlock MC. Compensatory mutations are repeatable and clustered within proteins. Proc R Soc B 2009;276: 1823–1827.
40. Poon A, Davis BH, Chao L. The coupon collector and the suppressor mutation: estimating the number of compensatory mutations by maximum likelihood. Genetics 2005;170:1323–1332.
41. Oria-Hernandez J, Rivero-Rosas H, Ramírez-Silva L. Dichotomic phylogenetic tree of the pyruvate kinase family: K+-dependent and -independent enzymes. J Biol Chem 2006;281:30717–30724.
42. Garza-Ramos G, Cabrera N, Saavedra-Lira E, Tuena de Gómez-Puyou M, Ostoa-Saloma P, Pérez-Montfort R, Gómez Puyou A. Sulfhydryl reagent susceptibility in proteins with high sequence similarity. Triosephosphate isomerase from *Tripanosoma brucei*, *Tripanosoma cruzi* and Leishmania mexicana. Eur J Biochem 1998;253: 684–691.
43. Saab-Rincón G, Olvera L, Olvera M, Rudiño-Piñera E, Benites E, Soberón X, Morett E. Evolutionary walk between $(\beta/\alpha)_8$ barrels: catalytic migration from triosephosphate isomerase to thiamine phosphate synthase. J Mol Biol 2012;416:255–270.
44. Gilles HM. Protozoan diseases. New York: Oxford University Press; 1999.
45. Sanchez-Ruiz JM. On promiscuity, changing environments and the possibility of replaying the molecular tape of life. Biochem J 2012; 445:e1–e3.
46. Breen S, Kemena C, Vlasov PK, Notredame C, Kondrashov FA. Epistasis as the primary factor en molecular evolution. Nature 2012; 490:533–538.